HEFAT2011
8th International Conference on Heat Transfer, Fluid Mechanics and Thermodynamics
11 – 13 July 2011
Pointe Aux Piments, Mauritius

DOUBLE-DIFFUSIVE NATURAL CONVECTION WITHIN A 3D POROUS ENCLOSURE, USING THE BOUNDARY ELEMENT METHOD

Kramer J.[1]*, Jecl R.[1], Ravnik J.[2], Škerget L.[2]
*Author for correspondence
[1]Faculty of Civil Engineering
[2]Faculty of Mechanical Engineering
University of Maribor,
Slovenia
E-mail: janja.kramer@uni-mb.si

ABSTRACT

A three-dimensional numerical study based on the boundary element method (BEM) was performed in order to study the problem of double-diffusive natural convection within a cubic enclosure filled with a fluid-saturated porous media, and subjected to horizontal temperature and concentration gradients. The fluid-flow within the porous media was modeled using space-averaged Navier-Stokes equations, coupled with energy and species equations. The used numerical algorithm is based on a combination of single domain and sub-domain BEM, and solves the velocity-vorticity formulation of the governing equations. The influences of the main controlling parameters, such as the porous Rayleigh number, Darcy number, Lewis number, and the buoyancy coefficient were investigated, by focusing on those situations, where the flow-field becomes 3D. The results for overall heat and solute-transfer through the porous enclosure are presented in terms of Nusselt and Sherwood numbers as functions of the governing parameters, and then compared to the numerical benchmarks published in literature.

INTRODUCTION

Problems of double-diffusive natural convection in porous media, resulting from the combined actions of temperature and concentration buoyancy forces, have been widely investigated over recent decades. Various important engineering problems within different fields can be modeled as an enclosure filled with porous media where the simultaneous occurrence of heat and mass-transfer can be investigated. Some practical examples of the problem include e.g. heat and moisture transport in fibrous insulation, groundwater-flow, contaminant transport through water-saturated soil, the heat and mass transfer within the mushy zone arising during the solidification of alloys. During such processes, complex flow-patterns may be formed,

NOMENCLATURE

c	[-]	Geometric coefficient
c	[J/kg K]	Heat capacity
C	[mol/m^3]	Species concentration
D	[m^2/s]	Mass diffusivity
Da	[-]	Darcy number
g	[m/s^2]	Gravity
K	[m^2]	Permeability
L	[m]	Characteristic length
Le	[-]	Lewis number
n	[-]	Normal vector
N	[-]	Buoyancy coefficient
p	[Pa]	Pressure
Pr	[-]	Prandtl number
Ra	[-]	Rayleigh number
r	[m]	Position vector
Sh	[-]	Sherwood number
t	[s]	Time
T	[K]	Temperature
u^*	[-]	Fundamental solution
v	[m/s]	Velocity

Special characters

α	[m^2/s]	Thermal diffusivity
β	[1/K]	Volumetric expansion coefficient
Γ	[-]	Boundary
λ	[W/m K]	Conductivity
ν	[m^2/s]	Kinematic viscosity
ξ	[-]	Source point
ρ	[kg/m^3]	Density
σ	[-]	Heat capacity ratio
ϕ	[-]	Porosity
ω	[1/s]	Vorticity
Ω	[-]	Domain

Subscripts

0	Reference state
e	Effective
f	Fluid phase
P	Porous
s	Solid phase
T	Thermal

mainly due to the presence of a porous media that adds hydraulic resistance, as well as competition between the thermal and concentration buoyancy forces.

The flow in porous enclosures under these circumstances was investigated mainly for two-dimensional geometry. However, for a certain range of controlling parameters within an enclosure imposed at thermal and concentration gradients, the flow may become 3D.

Several different configurations have been studied when considering double diffusive natural convection in porous enclosures which differ from each other regarding the positions of the thermal and concentration gradients. The most commonly studied configurations, which can be found in the literature are [1], [2]:

- thermal and concentration gradients are imposed on vertical walls and are either aiding or opposing each other,
- thermal and concentration gradients are imposed on horizontal walls and are either aiding or opposing each other,
- thermal/concentration gradient is imposed on a vertical wall and the concentration/thermal gradient is imposed on the horizontal wall.

Most published studies, dealing with double-diffusive natural convection in porous media are based on 2D geometry and mainly on situations where thermal and concentration buoyancy forces are aiding each other e.g. [3], [4], [5]. Only a few recent studies have considered 3D geometry. Sezai and Mohamad [6] published a study with 3D double-diffusive natural convection in porous media, where the thermal and concentration buoyancy forces are opposing each other. They reported that, under a certain range of controlling parameters e.g. the porous Rayleigh number, the Lewis number and the buoyancy coefficient, the flow in the cubic enclosure becomes 3D. Later, Mohamad et al. [7] investigated 3D convection flows in an enclosure subjected to opposing thermal and concentration gradients, focusing on the influence of the lateral aspect ratio. They found that, for a certain range of controlling parameters, the aspect ratio had no influence on the rates of heat and mass transfer, but strongly influences the flow structure.

This paper presents a numerical method for the simulation of double-diffusive natural convection within porous media, based on the boundary element method solution. The numerical algorithm is based on the combinations of single- domain and sub-domain boundary element methods, which solve the velocity-vorticity formulation of Navier-Stokes equations, written for porous media-flow. The proposed algorithm is based on pure fluid and nanofluid simulation codes as obtained by Ravnik et al. [8], [9].

MATHEMATICAL MODEL

The governing equations for the problem of double-diffusive natural convection in porous media are given in terms of conservation laws for mass, momentum, energy, and species. They are obtained from classical Navier-Stokes equations for the pure fluid-flow and are generally written at the microscopic level. Macroscopic or volume averaged Navier-Stokes equations can be derived by volume averaging over a suitably representative elementary volume (REV), and by considering the fact that only a part of this volume, expressed with the porosity ϕ, is available for fluid flow [10]. The macroscopic conservation equations can be written as:

- continuity equation:

$$\vec{\nabla}\vec{v} = 0 \tag{1}$$

- momentum equation:

$$\frac{1}{\phi}\frac{\partial \vec{v}}{\partial t} + \frac{1}{\phi^2}\left(\vec{v}\,\vec{\nabla}\right)\vec{v} = -\left(\beta_T\left(T-T_0\right)+\beta_C\left(C-C_0\right)\right)\vec{g} - \\ -\frac{1}{\rho}\vec{\nabla}p + \frac{1}{\phi}\nu\nabla^2\vec{v} - \frac{\nu}{K}\vec{v} \tag{2}$$

- energy equation:

$$\sigma\frac{\partial T}{\partial t} + \left(\vec{v}\,\vec{\nabla}\right)T = \frac{\lambda_e}{c_f}\nabla^2 T \tag{3}$$

- species equation:

$$\phi\frac{\partial C}{\partial t} + \left(\vec{v}\,\vec{\nabla}\right)C = D\nabla^2 C \tag{4}$$

The parameters used above are: $\vec{v}$ volume averaged velocity, ϕ porosity, t time, ρ density, ν kinematic viscosity, p pressure, $\vec{g}$ gravity vector, K permeability. In the energy equation, T is the temperature, σ represents the heat capacity ratio $\sigma = \left(\phi c_f + (1-\phi)c_s\right)/c_f$, where $c_f = \rho_f c_{pf}$, and $c_s = \rho_s c_{ps}$ are heat-capacities for the fluid and solid phases, respectively. λ_e is the effective thermal conductivity of the fluid-saturated porous media given as $\lambda_e = \phi\lambda_f + (1-\phi)\lambda_s$, where λ_f and λ_s are thermal conductivities for the fluid and solid phases, respectively. In the species equation, C is the concentration, and D the mass diffusivity.

In the model development, the following assumptions are adopted: the fluid flow is steady and laminar, the solid phase is homogeneous, isotropic, and non-deformable, the fluid is incompressible Newtonian, and in thermal equilibrium with the solid phase. The porosity and permeability of the porous medium are constant, whilst the density of the fluid only depends on the temperature and concentration variations, and is described using the Oberbeck-Boussinesq approximation as:

$$\rho = \rho_0\left(1-\beta_T(T-T_0)-\beta_C(C-C_0)\right) \tag{5}$$

where β_T is the volumetric thermal expansion coefficient, β_C is the volumetric expansion coefficient due to the chemical species, and the subscript 0 refers to a reference state. Furthermore, no internal energy sources are present in the fluid saturated porous media. The irreversible viscous dissipation is also neglected, whilst no high-velocity flow of highly-viscous fluid was considered in the present study. The solid phase of porous medium is assumed to be in thermal equilibrium with the saturating fluid.

The momentum equation (2) is also known as the Darcy-Brinkman equation, with two viscous terms e.g. the Brinkman viscous term (third on the r.h.s), and the Darcy viscous term

(fourth on the r.h.s.). The Brinkman viscous term is analogous to the Laplacian term in classical Navier-Stokes equations for pure fluid flow. It expresses the viscous resistance or viscous drag force exerted by the solid phase on the flowing fluid at their contact surfaces. The non-slip boundary condition on a surface which bounds porous media is satisfied with the Brinkman term [1].

Velocity-vorticity formulation

The proposed numerical algorithm is based on the boundary element method, which solves the velocity-vorticity formulations of Navier-Stokes equations. It can be derived by taking the curl of the mass conservation law (1) and of the Brinkman momentum equation (2). The vorticity is defined as the curl of the velocity field $\vec{\omega} = \vec{\nabla} \vec{v}$ and is solenoidal by the definition, $\vec{\nabla} \vec{\omega} = 0$. The computational scheme is consequently decoupled into kinematic and kinetic computational parts. The kinematics equation is a vector elliptic partial differential equation of the Poisson type, which links the velocity and vorticity fields for every point in space and time, and reads as:

$$\nabla^2 \vec{v} + \vec{\nabla} \times \vec{\omega} = 0 \tag{6}$$

Furthermore, the kinetic part is governed by the vorticity transport equation:

$$\begin{aligned} &\phi \frac{\partial \vec{\omega}}{\partial t} + \left(\vec{v} \vec{\nabla}\right) \vec{\omega} = \left(\vec{\omega} \vec{\nabla}\right) \vec{v} - \\ &- \phi^2 \vec{\nabla} \times \left(\beta_T \left(T - T_0\right) + \beta_C \left(C - C_0\right)\right) \vec{g} + \\ &+ \nu \phi \nabla^2 \vec{\omega} - \frac{\nu \phi^2}{K} \vec{\omega} \end{aligned} \tag{7}$$

Non-dimensional equations

Before all equations can be rewritten in non-dimensional form, in the vorticity, energy, and species equations the modified vorticity, temperature, and concentration time steps have to be introduced as $t \to t/\phi = t_\omega$, $t \to t/\sigma = t_T$, and $t \to t/\phi = t_C$. These are necessary mathematical steps allowing for to use of a numerical scheme, as presented in the following chapter.

The non-dimensional forms of governing equations are adopted, using the following dimensionless variables:

$$\begin{aligned} &\vec{v} \to \vec{v}/v_0, \vec{r} \to \vec{r}/L, t_\omega \to v_0 t_\omega/L, t_T \to v_0 t_T/L, \\ &t_C \to v_0 t_C/L, T \to \left(T - T_0\right)/\Delta T, \\ &C \to \left(C - C_0\right)/\Delta C, \vec{g} \to \vec{g}/g_0 \end{aligned} \tag{8}$$

v_0 is the characteristic velocity, $\vec{r}$ is the positional vector, and L the characteristic length. Furthermore, T_0 and C_0 are the characteristic temperature and concentration, ΔT and ΔC are the characteristic temperature and concentration differences and $g_0 = 9{,}81\, m/s^2$ is the gravity acceleration. The characteristic velocity is given by the expression $v_0 = \lambda_f / \left(\rho\, c_{pf}\right) L$. This choice for characteristic velocity is common for buoyant flow-simulations.

The macroscopic non-dimensional vorticity equation can now be written as:

$$\begin{aligned} &\frac{\partial \vec{\omega}}{\partial t_\omega} + \left(\vec{v} \vec{\nabla}\right) \vec{\omega} = \left(\vec{\omega} \vec{\nabla}\right) \vec{v} + \mathrm{Pr}\, \phi \nabla^2 \omega - \\ &- \mathrm{Pr}\, Ra_T \phi^2 \vec{\nabla} \times \left(T + N\, C\right) \vec{g} - \frac{\mathrm{Pr}}{Da} \phi^2 \vec{\omega} \end{aligned} \tag{9}$$

with the non-dimensional governing parameters defined as:

- Pr, Prandtl number:

$$\mathrm{Pr} = \frac{\nu}{\alpha} \tag{10}$$

where ν is the kinematic viscosity and α the thermal diffusivity given as $\alpha = \lambda_f / c_f$.

- Ra_T thermal fluid Rayleigh number:

$$Ra_T = \frac{g_0 \beta_T \Delta T L^3}{\nu \alpha} \tag{11}$$

- Da Darcy number:

$$Da = \frac{K}{L^2} \tag{12}$$

- N buoyancy coefficient:

$$N = \frac{Ra_C}{Ra_T} \tag{13}$$

- Ra_C solutal Rayleigh number:

$$Ra_C = \frac{g_0 \beta_C \Delta C L^3}{\nu \alpha} \tag{14}$$

The energy conservation equation in non-dimensional form can be written as:

$$\frac{\partial T}{\partial t_T} + \left(\vec{v} \vec{\nabla}\right) T = \frac{\lambda_e}{\lambda_f} \nabla^2 T \tag{15}$$

and finally the species conservation equation in non-dimensional form reads:

$$\frac{\partial C}{\partial t_C} + \left(\vec{v} \vec{\nabla}\right) C = Le \nabla^2 C \tag{16}$$

where Le is the Lewis number, given by the expression:

$$Le = \frac{\alpha}{D} \tag{17}$$

NUMERICAL METHOD

When considering a domain Ω with a boundary Γ, a fundamental solution of the Laplace equation and the Gauss and Greens' theorems are used to write the integral kinematics equation without the derivatives of the velocity or vorticity fields [11]:

$$\begin{aligned} &c\left(\vec{\xi}\right) \vec{v}\left(\vec{\xi}\right) + \int_\Gamma \vec{v} \left(\vec{n} \vec{\nabla}\right) u^* \, d\Gamma = \\ &= \int_\Gamma \vec{v} \times \left(\vec{n} \times \vec{\nabla}\right) u^* \, d\Gamma + \int_\Omega \left(\vec{\omega} \times \vec{\nabla} u^*\right) d\Omega \end{aligned} \tag{18}$$

Here $\vec{\xi}$ is the source or collocation point, $\vec{n}$ is the vector normal to the boundary, pointing out of the domain and u^* is the fundamental solution: $u^* = 1/4\pi\,|\vec{\xi} - \vec{r}\,|$. A tangential form of equation (18) is used in order to have a nonsingular system of equations for solving the boundary values of vorticity. It is obtained by a cross product with a unit normal, yielding:

$$\begin{aligned} & c\left(\vec{\xi}\right)\vec{n}\left(\vec{\xi}\right)\times\vec{v}\left(\vec{\xi}\right)+\vec{n}\left(\vec{\xi}\right)\times\int_{\Gamma}\vec{v}\,\vec{\nabla}\,u^*\vec{n}\,d\Gamma = \\ & =\vec{n}\left(\vec{\xi}\right)\times\int_{\Gamma}\vec{v}\times\left(\vec{n}\times\vec{\nabla}\right)u^*\,d\Gamma+\vec{n}\left(\vec{\xi}\right)\times\int_{\Omega}\left(\vec{\omega}\times\vec{\nabla}u^*\right)d\Omega \end{aligned} \tag{19}$$

The same fundamental solution and a standard BEM derivation are used to write the integral forms of the vorticity transport equation (9), the energy equation (15), and the species equation (16):

$$\begin{aligned} & c\left(\vec{\xi}\right)\omega_j\left(\vec{\xi}\right)+\int_{\Gamma}\omega_j\vec{\nabla}u^*\vec{n}\,d\Gamma=\int_{\Gamma}q_j u^*\,d\Gamma+ \\ & +\frac{1}{\mathrm{Pr}\,\phi}\int_{\Gamma}\vec{n}\left\{u^*\left(\vec{v}\,\omega_j-\vec{\omega}\,\vec{v}_j\right)\right\}d\Gamma- \\ & -\frac{1}{\mathrm{Pr}\,\phi}\int_{\Omega}\left(\vec{v}\,\omega_j-\vec{\omega}\,\vec{v}_j\right)\vec{\nabla}u^*d\Omega- \\ & -Ra_T\,\phi\left(\int_{\Gamma}\left(u^*T\vec{g}\times\vec{n}\right)_j\,d\Gamma\right)- \\ & -Ra_T\,\phi\left(\int_{\Omega}\left((T+N\,C)\,\vec{\nabla}\times u^*\vec{g}\right)_j d\Omega\right)+ \\ & +\frac{\phi}{Da}\int_{\Omega}\vec{\omega}u^*d\Omega \end{aligned} \tag{20}$$

$$\begin{aligned} & c\left(\vec{\xi}\right)T\left(\vec{\xi}\right)+\int_{\Gamma}T\vec{\nabla}u^*\vec{n}\,d\Gamma=\int_{\Gamma}q_T u^*\,d\Gamma+ \\ & +\frac{\lambda_f}{\lambda_e}\left(\int_{\Gamma}\vec{n}\left\{u^*\left(\vec{v}\,T\right)\right\}d\Gamma-\int_{\Omega}\left(\vec{v}\,T\right)\vec{\nabla}u^*d\Omega\right) \end{aligned} \tag{21}$$

$$\begin{aligned} & c\left(\vec{\xi}\right)C\left(\vec{\xi}\right)+\int_{\Gamma}C\,\vec{\nabla}u^*\vec{n}\,d\Gamma=\int_{\Gamma}q_C\,u^*\,d\Gamma+ \\ & +\frac{1}{Le}\left(\int_{\Gamma}\vec{n}\left\{u^*\left(\vec{v}\,C\right)\right\}d\Gamma-\int_{\Omega}\left(\vec{v}\,C\right)\vec{\nabla}u^*d\Omega\right) \end{aligned} \tag{22}$$

Here, ω_j is a vorticity component, q_j is a component of the vorticity flux, q_T is the heat-flux, and q_C is the species flux. In this present study, only steady flow-fields were considered, thus the time derivative terms $\partial\omega/\partial t_\omega$, $\partial T/\partial t_T$ and $\partial C/\partial t_C$ were omitted.

A combination of subdomain BEM and single-domain BEM for the solution of the governing equations was applied. The Dirichlet and/or Neumann boundary conditions for velocity, temperature and concentration were given. They were used to obtain solutions from the kinematics equation (18) for domain velocity values, energy equation (21) for the domain temperature values, and the species equation (22) for domain concentration values. The boundary conditions for vorticity, which are needed to solve the vorticity transport equation (20), were unknown. The single domain BEM on the tangential form of the integral kinematics equation (19) was used to obtain the unknown boundary vorticity values.

The outline of the algorithm is as follows:

- initialization, calculate integrals, set up parameters
- begin nonlinear loop
  - calculate boundary vorticity values by solving the tangential form of the kinematics equation (19) by single domain BEM
  - calculate domain velocity values by solving the kinematics equation (18) using subdomain BEM
  - solve the energy equation (21) using the new velocity field for domain temperature values by subdomain BEM
  - solve the species equation (22) using the new velocity field for domain concentration values by subdomain BEM
  - solve vorticity transport equation (20) by subdomain BEM for domain vorticity values using the boundary values from the solution of the kinematics equation, and the new velocity and temperature fields
  - check convergence - repeat steps in the nonlinear-loop until the convergence of all field functions is achieved
- end nonlinear loop
- output results

In the subdomain BEM method, which is used to solve equations (18), (20), (21) and(22) a mesh of the entire domain Ω is made, each mesh element is named as a subdomain. Equations are written for all source points on each of the subdomains. In order to obtain a discrete version, the integral equations shape functions are used to interpolate field functions and flux across the boundary and inside of the subdomain. In this work, hexahedral subdomains with 27 nodes were used, which enabled continuous quadratic interpolation of field functions. The boundary of each hexahedron consisted of 6 boundary elements. On each boundary element the flux was interpolated using a discontinuous linear interpolation scheme with 4 nodes. The flux definition problems in corners and edges could be avoided by using discontinuous interpolation. Between subdomains, the functions and their fluxes are assumed to be countinious. The resulting linear systems of equations were over-determined and sparse. They were solved in a least-squares manner. The discretization procedure for the single-domain BEM, which is used to solve equation (19), is analogous, with the distinction that source points are set into all the nodes along the boundary of the entire domain. The resulting linear system of equations is full. It is solved by the LU decompostion method. This algorithm is proposed for $3D$ fluid flow and heat transfer by Ravnik et al. [8]. The algorithm for simulations in porous media was expanded during this present work. The kinematics eqaution requires no changes,

whilst the porous parameters had to be introduced into the vorticity transport and energy equations. The Darcy term in the vorticity transport equation, which is absent in the pure fluid case, is linearly proportional to the unknown vorticity, thus it was included within the system matrix.

TEST CASES

The geometry under consideration was a cube enclosure, as shown in Fig.(1), filled with porous media, which was fully saturated with incompressible fluid. Left and right vertical walls were imposed onto different temperature and concentration values, where $T_1 > T_2$ and $C_1 > C_2$, whilst the remaining boundaries were adiabatic and impermeable.

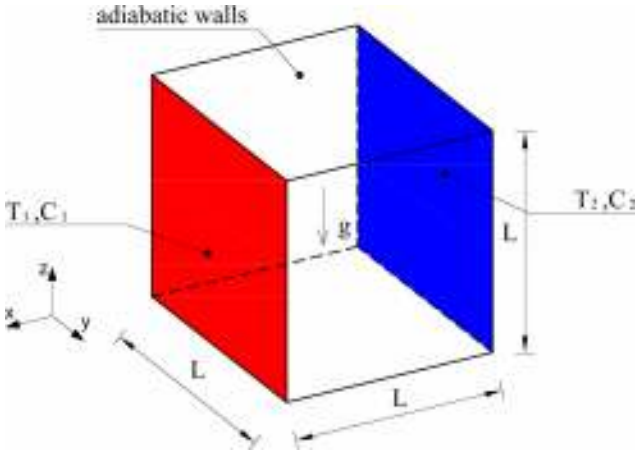

Figure 1 Geometry of the problem with boundary conditions

Natural convection phenomena within the enclosure will occur due to the subjected temperature and concentration differences on two vertical walls. The density of the heated fluid next to the hot wall decreases and the buoyancy will carry it upwards. On the other hand, fluid along the cold wall will be colder and denser and will travel downwards. Additional concentration buoyancy forces are induced due to applied concentration differences on the walls, which then cause additional movement of the fluid. Both induced buoyancy forces can aid or oppose each other, which also influences the strength of the fluid's convective motion. The cases where solute is transported due to induced temperature gradient (Soret effect) or heat is transfered due to concentration gradient (Dufour effect) were neglected in this present study.

Natural convection phenomena within a fluid-saturated porous medium is expected to be dependent on a number of parameters such as porosity, the thermal conductivity and heat capacity of the fluid, the solid phases, the viscosity of the fluid phase etc.. The wall heat and species fluxes were calculated for different values of Darcy number, the Lewis number, the buoyancy coefficient, and the porous Rayleigh number, which is defined as:

$$Ra_p = Ra_T Da = \frac{g_0 \beta_T \Delta T L K}{\nu \alpha} \tag{23}$$

The overall heat and mass flux through the cavity are expressed in terms of the average Nusselt and Sherwood numbers, given with eq. (24), where Γ is the surface through which the heat and species fluxes are calculated and $\vec{n}$ is the unit normal to this surface.

$$Nu = \int_{\Gamma} \vec{\nabla} T \, \vec{n} \, d\Gamma, \qquad Sh = \int_{\Gamma} \vec{\nabla} C \, \vec{n} \, d\Gamma \tag{24}$$

The calculations were performed on a non-uniform mesh with $20 \times 8 \times 20$ subdomains and $28{,}577$ nodes. Sub-domains were concentrated towards the hot and the cold walls. The convergence criteria for all the field functions was 10^{-5}, under-relaxation of vorticity, temperature and concentration values were used ranging from 0.1 to 0.01.

Firstly, the results are presented for the cases where the thermal buoyancy force was the only acting force $(Le = N = 0)$. Table (1) presents the Nusselt number values for the cubic enclosure for $\mathrm{Pr} = 0{,}71$, $\phi = 0{,}8$, $Ra_P = 1000$ and different values of Da. The results were compared to the study of authors R.V. Sharma and R.P. Sharma [12], where the $3D$ natural convection in a porous box is considered, and the fluid flow is modeled with the use of the Darcy-Brinkman-Forchheimer model. Very good agreement between the results was observed for the case of high Darcy number values $(Da = 10^{-4} \text{ - } 10^{-2})$. Slight differences occurred in the case of very low Darcy numbers $(Da = 10^{-5}$ and $10^{-6})$. In this case the effect of the Forchheimer term, which is excluded in the model of the present study, becomes significant and influences the overall heat transfer resulting in lower values of Nusselt numbers [12].

Ra_P / Da		10^{-1}	10^{-2}	10^{-3}	10^{-4}
1000	present	1.855	3.770	6.922	10.558
	[12]	-	3.99	6.95	10.14

Table 1 Nusselt number values for the $3D$ natural convection in a cube for $Ra_P = 1000$, and the different values of the Darcy number. The results are compared with the study of Sharma and Sharma [12].

In addition, Nusselt number values for natural convection for $\mathrm{Pr} = 0{,}71$, $\phi = 0{,}8$ $Ra_P = 50, 100, 200, 500, 1000$ and $10^{-6} < Da < 10^{-1}$ are presented graphically in Fig. (2). It can be observed, that the Nusselt number increased with any decrease in Da, and increase of Ra_P. The influence of the Darcy number was more pronounced at higher values of the porous Rayleigh number. At low values of Ra_P the Nusselt number values were near to 1, the dominant heat transfer mechanism in

this case being conduction. With increasing of Ra_P and the decreasing of Da, convection becomes dominant whilst conduction was negligible. When the values of Da were high, the Brinkman viscous term in the momentum equation played a significant role, and reduced the overall heat-transfer, which resulted in smaller values for Nu. With any decrease in Da, the influence of the Brinkman viscous term became almost negligible ($Da < 10^{-4}$). In this case the viscous effects became smaller and the inertial effects became significant due to high-fluid velocity. For low values of the Darcy number, the model gave similar results to the classical Darcy model [13].

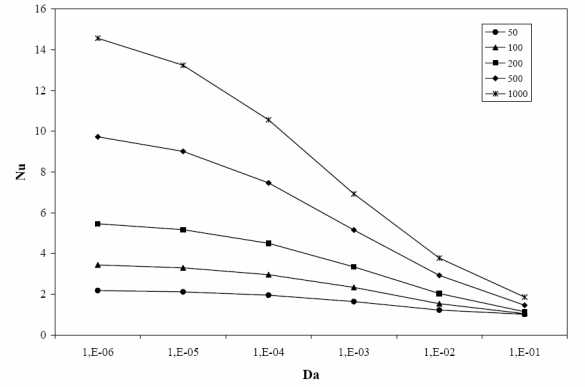

Figure 2 Dependence of the Nusselt number on the Darcy number for different values of porous Rayleigh number, in this case $Le = 0, N = 0$.

In addition, some results for double-diffusive natural convection are presented and compared with available results from the literature. Table (2) presents thr Nusslet and Sherwood number values for $Da < 10^{-6}$, and the different values of Ra_P, Le and N. A good agreement with the results from the study of Mohamad et al. [7] was obtained.

$Ra_P = 10, N = -0{,}5$	$Le = 1$	$Le = 10$
Nu	**1.019** (1.0198)	**1.039** (1.0404)
Sh	**1.019** (1.0198)	**2.450** (2.4467)
$Le = 50, N = -0{,}2$	$Ra_P = 1$	$Ra_P = 10$
Nu	**1.001** (1.0005)	**1.072** (1.0705)
Sh	**1.952** (1.9517)	**7.388** (6.9861)

Table 2 Nusselt and Sherwood number values for the $3D$ natural convection in a cube for $Da = 10^{-6}$ and different values of porous Rayleigh number, Lewis number and buoyancy coefficient. The results were compared to study of Mohamad et al. [7] (values in brackets).

Table (3) presents the results for double-diffusive natural convection, where $Le = 10$, $N = 1$. Thermal and solutal buoyancy forces aided each other, which resulted in higher heat-transfer and additional solute transfer through the porous enclosure, as can be observed from the values for Nusselt and Sherwood numbers.

Da	10^{-1}	10^{-2}	10^{-3}	10^{-4}	10^{-5}	10^{-6}
Nu	1.086	1.687	2.529	3.164	3.595	3.788
Sh	2.842	5.624	9.749	14.714	19.107	20.869

Table 3 Nusselt and Sherwood number values for $3D$ natural convection in a cube for $Ra_P = 100$, $Le = 10$, $N = 1$ and different values of porous Darcy number.

In Figures (3), (4) and (5) temperature and concentration contures on the plane $y = 0{,}5$ for $Ra_P = 100$, $Le = 10$, $N = 1$ and $Da = 10^{-2}, 10^{-4}, 10^{-6}$ are displayed together with velocity vectors.

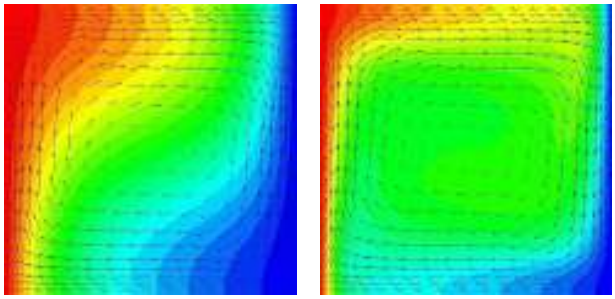

Figure 3 Temperature (left) and concentration (right) contour plots on the $y = 0{,}5$ plane for $Ra_P = 100$, $Da = 10^{-2}$, $Le = 10$ and $N = 1$.

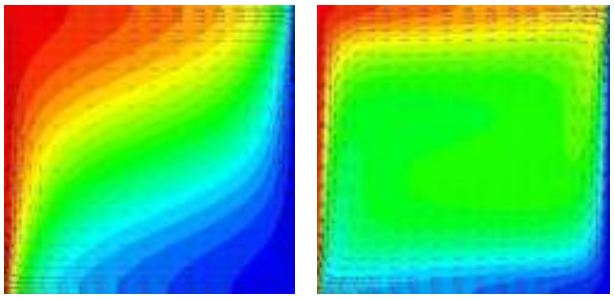

Figure 4 Temperature (left) and concentration (right) contour plots on the $y = 0{,}5$ plane for $Ra_P = 100$, $Da = 10^{-4}$, $Le = 10$ and $N = 1$.

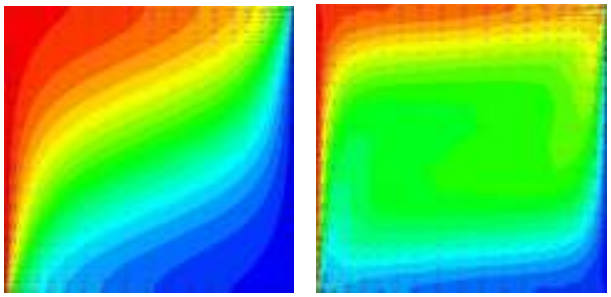

Figure 5 Temperature (left) and concentration (right) contour plots on the $y = 0{,}5$ plane for $Ra_P = 100$, $Da = 10^{-6}$, $Le = 10$ and $N = 1$.

Both fields were observed to be stratified in all cases, where layers of fluid with equal temperature and concentration were perpendicular to the direction of gravity, which was especially obvious within the central part of the cube. The temperature and concentration gradients increased with any decrease of the Darcy number. A higher Lewis number resulted in higher concentration gradients, as shown in the figures.

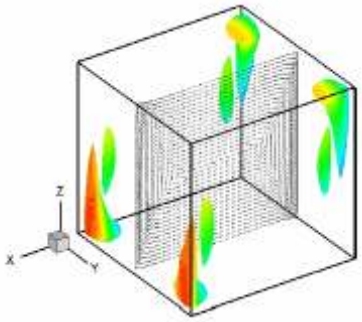

Figure 6 Iso-surfaces for $Ra_P = 500$, $Da = 10^{-3}$ and absolute value of velocity component $v_y = 3$. In addition, the velocity vectors on the plane $y = 0{,}5$ are displayed.

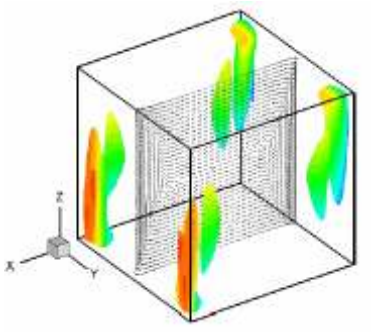

Figure 7 Iso-surfaces for $Ra_P = 1000$, $Da = 10^{-3}$ and absolute value of velocity component $v_y = 7$. In addition, the velocity vectors on the plane $y = 0{,}5$ are displayed.

Figs. (6) and (7) plot the iso-surfaces for the absolute value of the y velocity component. From the flow structure in the enclosure (velocity vectors), it can be seen that the flow-field is almost $2D$. This was due to the fact that the flow-field was driven by the temperature and concentration differences between the two opposite walls, which caused a large two-dimensional vortex in the y plane. The $3D$ nature of the phenomena can be observed in the corners of the domain, as shown in Figs. (6) and (7). The extent of the movement of the main vortex perpendicular to the plane is small, but it became more apparent in the case of higher Ra_P and lower values of Da, in general.

CONCLUSIONS

Three-dimensional double-diffusive natural convection in a cube enclosure filled with saturated porous media was examined numerically using the boundary element method. The numerical algorithm is based on a combination of the single domain and subdomain boundary element methods, which are used to solve the velocity-vorticity formulation of macroscopic Navier-Stokes equations. Some results for overall heat and solute transfer through enclosure are given in terms of Nusselt and Sherwood number values. The numerical results indicate, that the flow regime, as well as heat and solute transfer, strongly depend on the values of the governing non-dimensional parameters, e.g. the Rayleigh, Darcy and Lewis numbers. The 3D nature of the flow field is observed in the corners of the enclosure, although the fluid is moving predominantly within a single two-dimensional vortex.

ACKNOWLEDGMENTS

One of the authors (J. Kramer) acknowledges the financial support of the research project Z2-2035, as provided by the Slovenian Research Agency ARRS.

REFERENCES

[1] Nield, D.A. and Bejan, A., *Convection in porous media (Third edition)*, Springer, 2006.
[2] Vafai, K., *Handbook of porous media*, Taylor & Francis, 2005.
[3] Bejan, A. and Khair, K.R., Heat and mass transfer by natural convection in a porous medium, *International Journal of Heat and Mass Transfer,* 28:909-918, 1985.
[4] Alavyoon, F., On natural convection in vertical porous enclosures due to prescribed fluxes of heat and mass at the vertical boundaries, *International Journal of Heat and Mass Transfer,* 36:2479-2498, 1993.
[5] Goyeau, B, Songbe, J.P. and Gobin, D., Numerical study of double diffusive natural convection in a porous cavity using the Darcy-Brinkman formulation, *International Journal of Heat and Mass Transfer,* 39:1363-1378, 1996.
[6] Sezai, I. and Maohamad, A.A., Double diffusive convection in a cubic enclosure with opposing temperature and concentration gradient, *Physics of Fluids,* 12:2210-2223, 2000.
[7] Mohamad, A.A., Bennacer, R. and Azaiez, J., Double diffusion natural convection in a rectangular enclosure filled with binary fluid saturated porous media: The effect of lateral aspect ratio, *Physics of Fluids*, 16: 184-199, 2004.
[8] Ravnik, J., Škerget, L. and Žunič, Z.,Velocity-vorticity formulation for 3D natural convection in an inclined enclosure by BEM, *International Journal of Heat and Mass Transfer,* 51: 4517-4527, 2008.
[9] Ravnik, J., Škerget, L. and Hriberšek M., Analysis of three dimensional natural convection of nanofluids by BEM, *Engineering Analysis with Boundary Elements,* 34: 1018-1030, 2010.
[10] Bear, J., *Dynamics of fluids in porous media*, Dover Publications, Inc., New York, 1972.
[11] Škerget, L., Hriberšek, M. and Žunič, Z., Natural convection flows in complex cavities by BEM, *International Journal of Numerical methods for Heat&Fluid Flow*, 13: 720-735, 2003.
[12] Sharma, R.V. and Sharma, R.P., Non-Darcy effects on three-dimensional natural convection in a porous box. *Annals of the Assembly fot International Heat Transfer Conference,* 13, 2006.
[13] Jecl, R., Škerget, L., and Petrešin, E., Boundary domain integral method for transport phenomena in porous media, *International Journal for Numerical Methods in Fluids,* 35:39-54, 2001.